Metallomics

PAPER

View Article Online
View Journal

The effects of *pdr1*, *djr1.1* and *pink1* loss in manganese-induced toxicity and the role of α-synuclein in *C. elegans*

Cite this: DOI: 10.1039/c3mt00325f

Julia Bornhorst,†[ab] Sudipta Chakraborty,†[bc] Sören Meyer,[ad] Hanna Lohren,[a] Sigrid Große Brinkhaus,[e] Adam L. Knight,[f] Kim A. Caldwell,[f] Guy A. Caldwell,[f] Uwe Karst,[e] Tanja Schwerdtle,[a] Aaron Bowman[g] and Michael Aschner*[bhi]

Parkinson's disease (PD) is a neurodegenerative brain disorder characterized by selective dopaminergic (DAergic) cell loss that results in overt motor and cognitive deficits. Current treatment options exist to combat PD symptomatology, but are unable to directly target its pathogenesis due to a lack of knowledge concerning its etiology. Several genes have been linked to PD, including three genes associated with an early-onset familial form: *parkin*, *pink1* and *dj1*. All three genes are implicated in regulating oxidative stress pathways. Another hallmark of PD pathophysiology is Lewy body deposition, associated with the gain-of-function genetic risk factor α-synuclein. The function of α-synuclein is poorly understood, as it shows both neurotoxic and neuroprotective activities in PD. Using the genetically tractable invertebrate *Caenorhabditis elegans* (*C. elegans*) model system, the neurotoxic or neuroprotective role of α-synuclein upon acute Mn exposure in the background of mutated *pdr1*, *pink1* or *djr1.1* was examined. The *pdr1* and *djr1.1* mutants showed enhanced Mn accumulation and oxidative stress that was reduced by α-synuclein. Moreover, DAergic neurodegeneration, while unchanged with Mn exposure, returned to wild-type (WT) levels for *pdr1*, but not *djr1.1* mutants expressing α-synuclein. Taken together, this study uncovers a novel, neuroprotective role for WT human α-synuclein in attenuating Mn-induced toxicity in the background of PD-associated genes, and further supports the role of extracellular dopamine in exacerbating Mn neurotoxicity.

Received 1st November 2013,
Accepted 11th December 2013

DOI: 10.1039/c3mt00325f

www.rsc.org/metallomics

Published on 12 December 2013. Downloaded on 30/01/2014 17:07:09.

Introduction

Parkinson's disease (PD) is the second most common neurodegenerative disorder in the U.S., affecting nearly 1% of the population.[1]

With an age of onset typically around 60 years of age, this disease manifests a selective dopaminergic (DAergic) neuronal loss in the substantia nigra pars compacta (SNpc), resulting in overt motor and cognitive deficits.[2] The cardinal motor symptomatology of PD includes bradykinesia, rigidity, tremors and postural instability that may be preceded by emotional instability and cognitive problems.[3] As age remains the most significant risk factor for PD pathogenesis, the ever-increasing human lifespan has produced a financial and emotional burden worldwide. Untenable treatment options that do not target the etiology of PD are a major public health concern, and warrant further investigations into the specific mechanisms behind PD pathophysiology.

While the majority of PD cases are idiopathic, many genes have now been associated with the disease, including *DJ1*, *PINK1*, *parkin*, *NURR1*, *LRRK2*, *UCH-L1*, and *α-synuclein*.[3] The current study focuses on the major early-onset, familial PD genes: *parkin*, *pink1* and *dj1*. Homozygous mutations in the *PARK2*/*parkin* gene are responsible for nearly 50% of an autosomal recessive, early-onset, familial form of PD.[4] This gene encodes for an E3 ubiquitin ligase involved in the ubiquitin

[a] Institute of Food Chemistry, University of Münster, Münster, Germany
[b] Department of Pediatrics, Vanderbilt University Medical Center, Nashville, TN, USA
[c] Neuroscience Graduate Program, Vanderbilt University Medical Center, Nashville, TN, USA
[d] Graduate School of Chemistry, University of Münster, Münster, Germany
[e] Institute of Inorganic and Analytical Chemistry, University of Münster, Münster, Germany
[f] Department of Biological Sciences, University of Alabama, Tuscaloosa, AL, USA
[g] Department of Neurology, Vanderbilt Kennedy Center, Center for Molecular Toxicology, Vanderbilt University Medical Center, Nashville, TN, USA
[h] Department of Pharmacology, the Kennedy Center for Research on Human Development, and the Center for Molecular Toxicology, Vanderbilt University Medical Center, Nashville, TN, USA
[i] Department of Molecular Pharmacology, Albert Einstein College of Medicine, Forchheimer 209, 1300 Morris Park Avenue, Bronx, NY 10461, USA. E-mail: Michael.Aschner@einstein.yu.edu; Fax: +1 718 430 8922; Tel: +1 718 430 2317
† Both authors contributed equally to this study.

Published on 12 December 2013. Downloaded on 30/01/2014 17:07:09.

proteasome system (UPS) that targets substrates for degradation.[5] Mutations in this gene result in impaired ligase activity and substrate binding that can lead to increased protein aggregation.[6] *Parkin* knockout (KO) models show a variety of PD-associated phenotypes, including hypokinetic deficits, DAergic cell loss[7] and increased extracellular dopamine (DA) levels in the striatum.[8]

The PD-associated protein known as PINK1, or PTEN-induced kinase 1, is a mitochondrial-targeted protein that contains a highly conserved serine/threonine kinase domain.[9] Homozygous mutations in *PARK6/pink1* are also connected to autosomal recessive, early-onset PD.[10] These mutations typically result in impaired kinase activity[11] that is otherwise critical for maintaining mitochondrial integrity, as phosphorylation targets include mitochondrial fission and fusion factors,[12] as well as the mitochondrially-located serine protease HtrA2.[13] Wildtype PINK1 has been shown to protect against mitochondrial toxin-induced DAergic cell death, as well as reducing apoptotic caspase levels and mitochondrial cytochrome *c* release.[14] *pink1* mutants show increased DAergic cell death[15] and impaired DA release.[16]

Recent studies have identified parkin as a PINK1 phosphorylation target. In fact, these two proteins work in parallel to promote mitophagy through a PINK1-mediated phosphorylation (and autophosphorylation) and recruitment of parkin to mitochondria with a lowered membrane potential.[17] Various modulators of this interaction have recently been introduced, including the mitochondrial fusion factor Mitofusin 2 (Mtfn2) and voltage-dependent anion channels (VDACs).[18] This novel role for both parkin and PINK1 reveals the importance of maintaining proper mitochondrial trafficking and turnover, signifying an impaired clearance of defective mitochondria as a potential mechanism in the pathophysiology of PD.

Additionally, mutations in the *PARK7/dj1* gene are also associated with autosomal recessive, early-onset PD.[19] This gene encodes for a protein that functions as an oxidative stress sensor, where oxidation of a cysteine residue results in translocation of the acidic isoform from the cytoplasm to the mitochondria.[20] Mutations in *dj1* result in increased ROS levels, impaired mitochondrial energetics[21] and DAergic cell death, while overexpression protects against DA toxicity and cell loss.[22] DJ1 has also been shown to form a multi-protein complex with parkin and PINK1,[23] though this remains controversial. Moreover, DJ1 up-regulation can reduce the loss of PINK1-mediated sensitization of DAergic neurons in the SNpc to a mitochondrial toxin.[24] The reduction of *pink1* loss-mediated mitochondrial deficits by DJ1 was also seen in *Drosophila*, but no reduction was seen in *parkin* mutants.[25] These data reveal the role of DJ1 acting in parallel with the parkin/PINK1 pathway.

Another gene implicated in PD pathophysiology is *SNCA*[26] that encodes for α-synuclein (α-Syn), the major aggregated component of Lewy body depositions. Pathogenic mutations in the *SNCA* gene have been shown to promote increased aggregation of the protein.[27] While the function of α-Syn remains unclear, high expression is found in neuronal presynaptic terminals. Recent evidence has implicated α-Syn in regulating synaptic vesicle release, mobility and recycling,[28] along with decreased DA release from vesicles in the background of α-Syn overexpression.[29] Wildtype α-Syn has been shown to inhibit tyrosine hydroxylase (TH) activity, suggesting a physiological role in controlling optimal DA biosynthesis.[30] However, aggregated forms are no longer able to inhibit TH activity, with higher TH phosphorylation present.[31] Elucidating the role of wildtype α-Syn in the background of other PD genes may provide deeper insight into the neuroprotective or neurotoxic nature of α-Syn in PD.

While genes such as *SNCA*, *parkin*, *pink1* and *dj1* may be associated with PD, the heterogeneity in age-of-onset, as well as 90% of cases being sporadic in nature, warrants investigation into the role of environmental factors in PD etiology. One such factor is manganese (Mn). This is an essential trace element that is necessary for proper immune function, bone growth, digestion, reproduction, as well as for serving as an important cofactor for many enzymes.[32] However, overexposure can result in symptomatology that resembles PD.[33] Environmental sources of Mn exposure can include drinking water (groundwater), pesticides, manufacturing by-products, and airborne exposure upon combustion of the fuel additive methylcyclopentadienyl manganese tricarbonyl (MMT). However, excessive occupational Mn exposure may also arise from welding, steel mining, smelting, and other industrial occupations.[34] Several studies have already begun to examine gene–environment interactions between Mn exposure and PD-associated genes. For example, rats exposed to Mn-containing welding fumes show an increase in parkin protein levels;[35] parkin was also shown to selectively protect against Mn-induced DAergic cell death *in vitro*.[36]

In this work, the tractable, invertebrate *Caenorhabditis elegans* (*C. elegans*) model system expressing human wildtype α-Syn was used for the first time to examine the roles of several early-onset, PD-associated genes (*pdr1*, *pink1* and *djr1.1*) and α-Syn in mediating Mn-induced neurotoxicity. Thereby, Mn uptake and Mn-induced oxidative stress in the background of mutated *pdr1*, *pink1* and *djr1.1* are illustrated. Furthermore, this paper demonstrates a novel role for α-Syn in altering Mn accumulation in the background of mutated genes (*pdr1* and *djr1.1*) through the utilization of inductively coupled plasma-mass spectrometry (ICP-MS/MS), as well as visualizing intra-worm Mn levels using laser ablation-inductively coupled plasma-mass spectrometry (LA-ICP-MS).

Experimental

C. elegans strains and handling

C. elegans strains were handled and maintained at 20 °C as previously described.[37] The following control strains were used: N2, *wildtype* (*Caenorhabditis* Genetics Center, CGC); and BY200, $p_{dat\text{-}1}$::GFP(*vtIs1*) *V* (kindly provided by the Blakely laboratory, Vanderbilt University Medical Center). The following deletion mutants were used: VC1024, *pdr1(gk448) III* (CGC); *pink1*(*tm1779*) *II*; and *djr1.1*(*tm918*) *II*. These deletion strains were also crossed with the BY200 strain for GFP control studies. The following

 This journal is © The Royal Society of Chemistry 2014

Published on 12 December 2013. Downloaded on 30/01/2014 17:07:09.

α-synuclein-containing strains were kindly provided by the Caldwell laboratory (University of Alabama): UA44, $p_{dat\text{-}1}$::α-syn, $p_{dat\text{-}1}$::GFP[*baIn11*]; UA88, *pdr1*(*tm598*), $p_{dat\text{-}1}$::α-syn, $p_{dat\text{-}1}$::GFP[*baIn11*]; UA84, *djr1.1*(*tm918*), $p_{dat\text{-}1}$::α-syn, $p_{dat\text{-}1}$::GFP[*baIn11*]; and UA86, *pink-1*(*tm1779*); $p_{dat\text{-}1}$::GFP, $p_{dat\text{-}1}$::α-syn [*baIn11*].

Preparation of $MnCl_2$

$MnCl_2$ (>99.995% purity) (Sigma-Aldrich) stock solutions were prepared in 85 mM NaCl. To prevent oxidation, fresh stock solutions were prepared shortly before each experiment.

Acute Mn treatments and Mn-induced lethality assay

2500 synchronized L1 worms per tube were acutely exposed to $MnCl_2$ in triplicate in siliconized tubes for 30 minutes. Worms were then pelleted by centrifugation at 7000 rpm for 3 minutes and washed four times in 85 mM NaCl. 30–50 worms were then pre-counted and transferred onto OP50-seeded NGM plates and blinded. The total number of surviving worms was scored 48 hours post-treatment.

Mn quantification in *C. elegans*

Mn content was determined after ashing of L1 worms by ICP-MS/MS. Briefly, 50 000 synchronized L1 worms were acutely treated with $MnCl_2$. Worms were pelleted, washed five times in 85 mM NaCl and re-suspended in 1 mL 85 mM NaCl supplemented with 1% protease inhibitor. After sonication, an aliquot was taken for protein quantification using the bicinchoninic acid (BCA) assay-kit (Thermo Scientific). Subsequently, the suspension was mixed again, evaporated, and incubated with the ashing mixture (65% HNO_3/30% H_2O_2 (1/1) (both from Merck)) at 95 °C for at least 12 h. After dilution of the ash with 2% HNO_3 including 10 μg L^{-1} Rh as internal standard to compensate drift effects, the Mn concentration was determined using ICP-MS/MS (Agilent 8800 ICP-QQQ). The nebulizer gas flow and parameters of lenses, Q1, collision cell and Q2 were tuned daily on a daily basis for maximum sensitivity (an oxide ratio of $<1.0\%$ ($^{140}Ce^{16}O^+/^{140}Ce+$) and a double charged ratio of $<1.5\%$ ($^{140}Ce++/^{140}Ce+$) with background counts of <0.1 cps (Table 1). The limit of quantification (LOQ) for Mn was 0.10 μg L^{-1} calculated according to the 3σ-criterion.[38] Determinations of blank and certified reference material (CRM 414 (plankton) (Community Bureau of Reference of the Commission of the European Communities)) were performed periodically after 15 samples each.

Table 1 Conditions for ICP-MS/MS (Agilent 8800 ICP-QQQ)

Power	1550 W
Plasma gas	15 L min^{-1}
Carrier gas	1.0 L min^{-1}
Auxiliary gas	0.9 L min^{-1}
Scan mode	Single quad
Q1	Ion guide
Collision cell gas flow	He: 4.5 mL min^{-1} (purity: >99.999%)
	H_2: 0.5 mL min^{-1} (purity: >99.999%)
Q2	^{55}Mn, ^{103}Rh (ISTD)
Integration time	1.0 s
Replicates	5

Table 2 Conditions for ICP-MS (ICAP Qc, Thermo Fisher Scientific)

Power	1550 W
Nebulizer flow	780 mL min^{-1}
Cool flow	14.0 L min^{-1}
Auxiliary flow	500 mL min^{-1}
Measurement mode	KEDS
Cell gas flow	4.6 mL min^{-1}

Additionally, the Mn content was qualitatively confirmed by LA-ICP-MS analyses. Briefly, 50 000 synchronized L1 worms acutely exposed to $MnCl_2$ were pelleted and washed three times with 85 mM NaCl and two times with bidistilled water. Worms were prepared for analyses by drying single worms on microscopic slides (Thermo Scientific).

The laser ablation system LSX213G2+(CETAC Technologies) was coupled to an ICP-MS (ICAP Qc, Thermo Fisher Scientific). Slides were placed in the ablation chamber and ablated linewise using a quintupled Nd:YAG laser (wavelength 213 nm, repetition frequency 20 Hz spot, spot diameter 4 μm). The ablated material was transported into the ICP-MS by the carrier gas (He/Ar) and analytes were determined using the MS in KEDS mode (Tables 2 and 3). In addition, a 10 μg L^{-1} Rh-solution including 2% HNO_3 was continuously delivered into ICP *via* a cyclonic spray chamber to compensate for drift effects during analysis.

Dopaminergic degeneration assay

Synchronized L1 worms (2500 per tube) were acutely exposed to $MnCl_2$. Upon washing, all worms were plated on OP50-seeded NGM plates. Forty-eight hours post-treatment, 50 worms were transferred to fresh OP50-seeded NGM plates and blinded for subsequent imaging. At 72 hours post-treatment, 15 worms per condition were mounted onto 4% agar pads (in M9 buffer) and anesthetized with 0.2% tricaine/0.02% tetramisole in M9 buffer. Scoring of neuronal defects was performed using an epifluorescence microscope (Nikon Eclipse 80i) equipped with a Lambda LS Xenon lamp (Sutter Instrument Company) and Nikon Plan Fluor 20× dry and Nikon Plan Apo 60× 1.3 oil objectives. Each worm was scored for the absence (''normal'') or presence of any of the following morphological changes: puncta formation along dendritic processes; shrunken soma; and/or loss of soma and/or dendrites (''degenerated''). Representative confocal images (Carl Zeiss MicroImaging, Inc.) of each morphological phenotype were taken and processed as previously described.[39]

RONS measurements

The formation of reactive oxygen and nitrogen species (RONS) in whole L1 worms was evaluated by a 5(&6)-carboxy-2′,7′-dichlorodihydrofluorescein-diacetate (carboxy-DCFH-DA)-based plate reader

Table 3 Conditions for LA (LSX213G2+, CETAC Technologies)

Repetition frequency	20 Hz
Spot diameter	4 μm
Scan rate	4 μm s^{-1}
He-flow 1	500 mL min^{-1}
He-flow 2	300 mL min^{-1}
Additional Ar-flow	400 mL min^{-1}

Published on 12 December 2013. Downloaded on 30/01/2014 17:07:09.

system. Briefly, a carboxy-DCFH-DA stock solution (50 mM in DMSO) (Invitrogen) was diluted 1 : 100 with M9 buffer, and synchronized L1 worms were exposed to 500 μM for 1 h in the dark. After 1 h, the worms were washed two times with M9 buffer and two times with 85 mM NaCl to remove all the carboxy-DCFH-DA content outside the worms. 10 000 worms were transferred to each well of a 96-well plate and incubated with H_2O_2 (positive control) or $MnCl_2$ (respective LD_{25} concentration). Immediately after incubation, the intracellular oxidation of carboxy-DCFH, which correlates with intracellular RONS, was monitored (excitation 485 nm/emission 535 nm) by a microplate reader (FLUOstar Optima microplate reader, BMG Labtechnologies), and kinetics were constructed up to 420 min. To exclude interfering fluorescence of the matrix, data were normalized to a control (dye-loaded cells without a RONS generator).

Glutathione quantification

Total intracellular glutathione levels (reduced and oxidized GSH) were determined using the ''enzymatic recycling assay'', as previously described.[40] Briefly, whole worm extracts were prepared out of 50 000 L1 worms acutely exposed to $MnCl_2$. This was followed by washing with 85 mM NaCl and sonication of the pellet in 0.1 mL ice cold extraction buffer (1% Triton X-100, 0.6% sulfosalicylic acid) and 1% protease inhibitor in KPE buffer (0.1 M potassium phosphate buffer, 5 mM EDTA). Intracellular GSH was quantified by measuring the change in absorbance per minute at 412 nm by a microplate reader after reduction of 5,5′-dithio-2-nitrobenzoic acid (DTNB, Sigma-Aldrich).

TaqMan gene expression assay

Total RNA was isolated *via* the Trizol method. Briefly, following treatment, 1 mL of Trizol (Life Technologies) was added to each tube containing worms resuspended in 100 μL 85 mM NaCl, followed by three cycles of freezing in liquid nitrogen and thawing at 37 °C. 200 μL of chloroform was then added to each tube, followed by precipitation using isopropanol and washing with 75% ethanol. Following isolation, 1 μg total RNA was used for cDNA synthesis using the High Capacity cDNA Reverse Transcription Kit (Life Technologies), as per manufacturer's instructions. cDNA samples were stored at 4 °C. Quantitative real-time PCR (BioRad) was conducted in duplicate wells using TaqMan Gene Expression Assay probes (Life Technologies) for each gene, using the *afd-1* (*actin* homolog) housekeeping gene for normalization after determining the fold difference using the comparative $2^{-\Delta\Delta Ct}$ method.[41] The following probes were used: human *dat-1* (assay ID: Ce02450891_g1); *skn-1* (assay ID: Ce02407447_g1); and *afd-1* (assay ID: Ce02414573_m1).

Statistics

Dose–response lethality curves and all histograms were generated using GraphPad Prism (GraphPad Software Inc.). A sigmoidal dose–response model with a top constraint at 100% was used to draw the lethality curves and determine the respective LD_{50} values (values represent the respective Mn concentrations that induce 50% reduction in survival), followed by a one-way analysis of variance (ANOVA) with a Dunnett's post-hoc test to compare all strains to their respective control strains. In order to compare all α-Syn to non-α-Syn-containing strains, a one-way ANOVA using Bonferroni's multiple comparison *post-hoc* test was conducted. Two-way ANOVAs were performed on the metal content, RONS, GSH and TaqMan gene expression data, followed by Bonferroni's multiple comparison post-hoc tests. Degeneration data were plotted as a stacked histogram and analyzed using an unpaired *t*-test between groups (*vs.* respective control strains).

Results

pdr1 mutants are hypersensitive to acute Mn exposure

Assessment of dose–response survival curves following acute Mn exposure revealed a leftward-shift in the curve for *pdr1* mutant worms compared to N2 wild-type (WT) worms (Fig. 1A).

Thus, *pdr1* mutants exhibited hypersensitivity to Mn-induced lethality (LD_{50} = 5.59 mM) compared to WT worms (LD_{50} = 10.43 mM). *djr1.1* mutants were less sensitive to acute Mn exposure *vs.* WT worms. *djr1.1*, one of the two djr-orthologues, shows the highest homology to vertebrate *dj1* and broadest expression (similar to the other deletion mutants).[42] Therefore, all studies were carried out in the *djr1.1* orthologue. Treating worms containing human WT α-Syn in addition to the respective genetic deletions (*pdr1*, *pink* and *djr1.1*) with Mn led to increased sensitivity compared to the WT α-Syn control strain (Fig. 1B). One-way ANOVA analysis (comparing data from Fig. 1A and B) showed a significantly increased sensitivity of the α-Syn-containing *djr1.1* mutants towards Mn compared to the *djr1.1* mutants alone (Fig. 1C).

Enhanced Mn accumulation in *pdr1* and *djr1.1* mutants is attenuated by WT α-Syn expression

To determine whether a genetic deletion and/or the presence of WT α-Syn alters Mn bioavailability in *C. elegans*, the Mn content was measured by ICP-MS/MS. Overall, the analyzed strains (Fig. 2A and B) showed a dose-dependent increase in the Mn content (two-way ANOVA, concentration $p < 0.0001$). The *pdr1* and *djr1.1* deletion mutants exhibited an enhanced Mn accumulation compared to WT worms (Fig. 2A). *pink1* mutants showed Mn accumulation that was indistinguishable from WT worms (Fig. 2A). Notably, the *pdr1* and *djr1.1* mutants containing α-Syn accumulated less Mn compared to the respective deletion mutants alone (Fig. 2C and D). While the reduction effect was not significant for the *pdr1* mutants (Fig. 2C), the decrease in accumulation was significant at 7.5 and 10 mM Mn for the *djr1.1* mutants (Fig. 2D). Moreover, we qualitatively confirmed the intraworm Mn accumulation using LA-ICP-MS. WT and *djr1.1* mutants, with and without α-Syn, were treated acutely with LD_{50} dose (10 mM) (Fig. 1). The images corroborate the ICP-MS/MS metal content analyses, showing increased Mn accumulation in the *djr1.1* mutants compared to the α-Syn-containing *djr1.1* mutants (Fig. 2E).

 This journal is © The Royal Society of Chemistry 2014

Published on 12 December 2013. Downloaded on 30/01/2014 17:07:09.

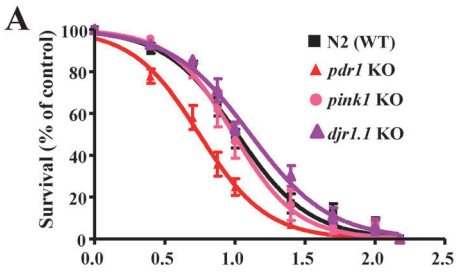

Strain	LD_{50} (mM)
N2 (WT)	10.43
pdr1 KO	5.59 **
pink1 KO	9.85
djr1.1 KO	12.93 **

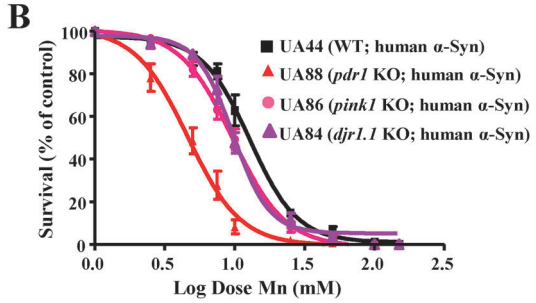

Strain	LD_{50} (mM)
UA44 (WT; human α-Syn)	12.82
UA88 (*pdr1* KO; human α-Syn)	4.63 **
UA86 (*pink1* KO; human α-Syn)	9.70 **
UA84 (*djr1.1* KO; human α-Syn)	9.74 **

C

Strain	Statistical significance
N2 (WT) vs. UA44 (WT; human α-Syn)	ns
pdr1 KO vs. UA88 (*pdr1* KO; human α-Syn)	ns
pink1 KO vs. UA86 (*pink1* KO; human α-Syn)	ns
djr1.1 KO vs. UA84 (*djr1.1* KO; human α-Syn)	*

Fig. 1 *pdr1* mutants are hypersensitive to an acute Mn exposure. (A, B) Dose–response survival curves following acute Mn exposure and the respective LD_{50} doses. All values were compared to non-treated worms set to 100% survival and plotted against the logarithmic scale of the used Mn concentrations. (A) N2 (wildtype, WT) and *pdr1*, *pink1* and *djr1.1* deletion mutants were treated for 30 min at L1 (larval) stage with increasing concentrations of $MnCl_2$. (B) UA44 (WT; human α-Syn), UA88 (*pdr1* KO; human α-Syn), UA86 (*pink1* KO; human α-Syn) and UA84 (*djr1.1* KO; human α-Syn) were treated for 30 min at L1 stage with increasing concentrations of $MnCl_2$. (A, B) Data are expressed as means ± SEM from at least four independent experiments. Statistical analysis of the LD_{50}: $^{**}p < 0.01$ *versus* respective wildtype worms. (C) Statistical comparison of respective non-α-Syn and α-Syn containing worms: $^{*}p < 0.05$. KO = deletion mutants.

Absence of Mn-induced DAergic neurodegeneration

Next, we determined whether the aforementioned Mn concentrations induce dopaminergic (DAergic) neurodegeneration. Visualization of the architecture of the four cephalic (CEP) DAergic neurons in the head was performed using worms expressing the green fluorescent protein (GFP) under the control of a promoter for the dopamine re-uptake transporter 1 (*C. elegans* orthologue for vertebrate DAT[43]), $p_{dat\text{-}1}$::GFP (*vtIs1*). Using an objective scoring system, the CEP neurons were scored as degenerated if they exhibited any of the following: discontinuous, punctated GFP signal in the dendrites (3A, II); shrinkage of the cell body (3A, III); and/or, ultimately, total loss of soma and/or dendritic GFP signal (Fig. 3A, IV). Mn treatment did not significantly increase the inherent DAergic neurodegeneration in WT worms and deletion mutants (Fig. 3B, a–c). Assessment of neurodegeneration at 24 and 48 hours post-treatment (larval stages) also showed no change in DAergic neurodegeneration (data not shown). However, the α-Syn-containing *pdr1* deletion mutants show a reduction in the degeneration of the CEP architecture, while the α-Syn-containing *djr1.1* deletion mutants do not.

Mn-induced oxidative stress is exacerbated in *pdr1* and *djr1.1* mutants, but reduced by α-Syn expression

Oxidative stress is implicated in Mn-induced neurotoxicity.[44] Additionally, *parkin*, *pink* and *dj1* are all involved in regulating oxidative stress pathways.[45] Therefore, we investigated the relationship between Mn, oxidative stress and defense responses by measuring the presence of RONS and total GSH levels. To determine the presence of RONS in whole worms, a carboxy-DCFH-DA based reader test system was established (data not shown). Fig. 4A shows Mn-induced RONS levels in WT worms, *pdr1* and *djr1.1* mutants, along with their respective α-Syn-expressing strains. In response to sub-lethal, acute Mn treatment (respective LD_{25}), WT worms showed a time-dependent increase in Mn-induced RONS that was exacerbated in *pdr1*, p*ink1* and *djr1.1* mutants (data are normalized to the respective controls (dye-loaded cells without a RONS generator) at each respective timepoint). As illustrated in Fig. 4A (c and d), *pdr1* and *djr1.1* mutants containing α-Syn showed a lower Mn-induced RONS level compared to the non-α-Syn expressing deletion mutants.

Next, GSH levels were analysed in the deletion mutants to ascertain their redox status. The deletion mutants contained significantly less total GSH than WT worms (Fig. 4B). Mn treatment resulted in a slight reduction in GSH levels, which did not attain statistical significance. The significant decrease in GSH levels at 10 mM Mn in the *pdr1* mutants likely reflects Mn-induced lethality at this dose (Fig. 1A). The α-Syn-containing deletion mutants showed similar effects as the deletion mutants alone (data not shown). Treatment with H_2O_2 as a positive control corroborated that the inherently decreased levels of GSH in the mutants represent an innately defective oxidative stress response, as H_2O_2 treatment did not significantly alter GSH levels from baseline levels as compared to WT worms (data not shown).

Increased *skn-1* mRNA expression in *djr1.1* and *pink1* mutants

To determine whether the differences in oxidative stress levels are associated with differences in cellular defense responses against oxidative stress, expression of the antioxidant response gene *skn-1*, the orthologue of the vertebrate gene *nrf2*,[46] was examined. Gene expression data reveal inherently upregulated *skn-1* mRNA levels in the deletion mutants compared to WT

Published on 12 December 2013. Downloaded on 30/01/2014 17:07:09.

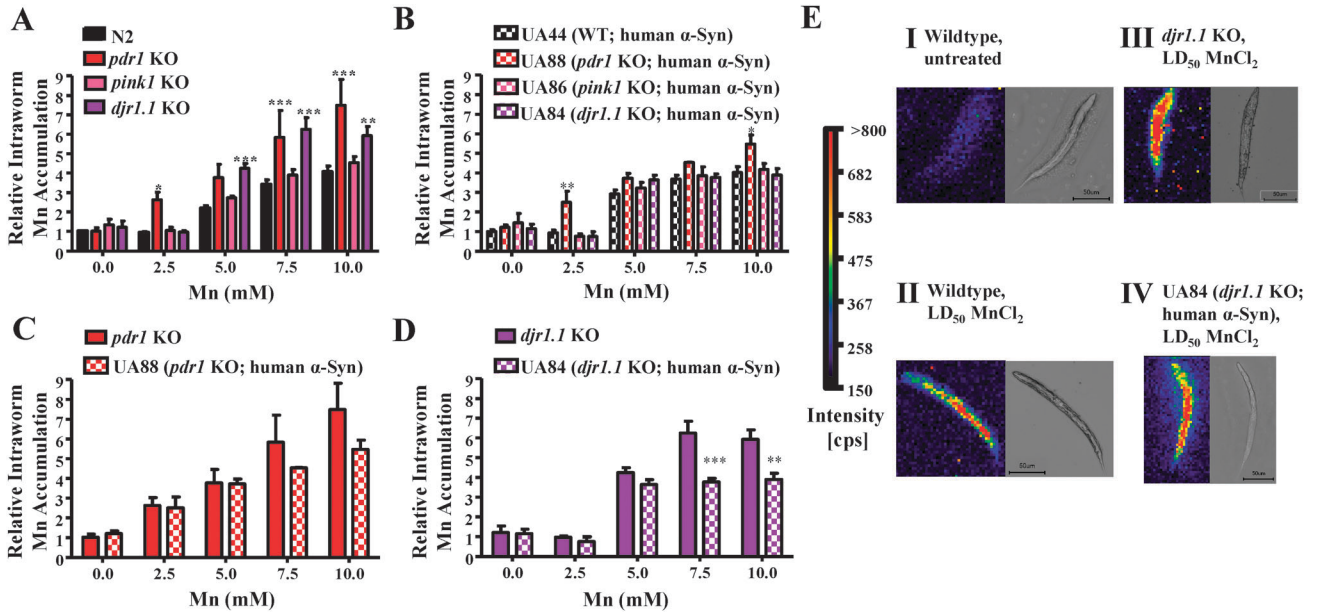

Fig. 2 Enhanced Mn accumulation in *pdr1* and *djr1.1* mutants is reversed by WT α-Syn expression. (A–D) Intraworm Mn content after acute treatment with $MnCl_2$ was quantified by ICP-MS/MS. All values were normalized to non-treated wildtype (WT) worms. (A) N2 (WT) and *pdr1*, *pink1* and *djr1.1* deletion mutants were treated at L1 stage for 30 min with increasing concentrations of $MnCl_2$. (B) UA44 (WT; human α-Syn), UA88 (*pdr1* KO; human α-Syn), UA86 (*pink1* KO; human α-Syn) and UA84 (*djr1.1* KO; human α-Syn) were treated at L1 stage for 30 min with increasing concentrations of $MnCl_2$. (C) Comparing intraworm Mn content of *pdr1* mutants and UA88 (*pdr1* KO; human α-Syn) after 30 min treatment with $MnCl_2$ (data from A, B). (D) Comparing intraworm Mn content in *djr1.1* mutants and UA84 (*djr1.1* KO; human α-Syn) after 30 min treatment with $MnCl_2$ (data from A, B). (A–D) Data are expressed as means + SEM from at least six independent experiments. Statistical analysis using two-way ANOVA: (A) interaction $p < 0.001$, genotype $p < 0.001$, concentration $p < 0.001$; (B) interaction ns, genotype $p < 0.001$, concentration $p < 0.001$; (C) interaction ns, genotype ns, concentration $p < 0.001$; (D) interaction $p < 0.001$, genotype $p < 0.001$, concentration $p < 0.001$. ***$p < 0.001$, **$p < 0.01$, *$p < 0.05$. (E) 2D images and respective microscopy images of WT worms (I, non-treated; II, 10 mM $MnCl_2$); *djr1.1* deletion mutants (III) and UA84 (*djr1.1* KO; human α-Syn) (IV) incubated with 10 mM $MnCl_2$ for 30 min. KO = deletion mutants; ns = not significant.

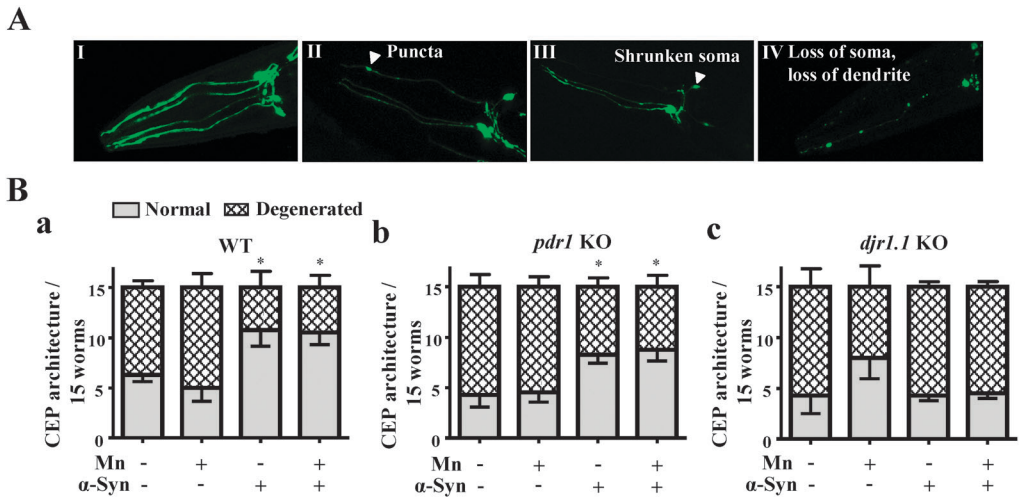

Fig. 3 Absence of Mn-induced DAergic neurodegeneration. (A) Representative confocal images used in the scoring system: normal worms (I), worms showing puncta (II), shrunken soma (III) or loss of dendrites and soma (IV). (B) The CEP architecture of 15 worms per group of WT, *pdr1* and *djr1.1* mutants and the respective α-Syn-containing strains (UA44, UA86, UA88) were scored 72 hours after an acute, 30 min treatment with $MnCl_2$. Shown are mean values + SEM of at least four experiments each. *$p < 0.05$ *versus* respective non-treated worms without α-Syn. KO = deletion mutants; ns = not significant.

worms (Fig. 5A), reaching statistical significance in the *pink1* and *djr1.1* mutants. Acute Mn treatment resulted in an upregulation of *skn-1* mRNA at the LD_{50} dose only in *djr1.1* mutants. Interestingly, the *pdr1* mutants containing α-Syn showed a trend for increased *skn-1* mRNA expression, whereas the levels were decreased in the *pink1* and *djr1.1* mutants (Fig. 5B).

 This journal is © The Royal Society of Chemistry 2014

Published on 12 December 2013. Downloaded on 30/01/2014 17:07:09.

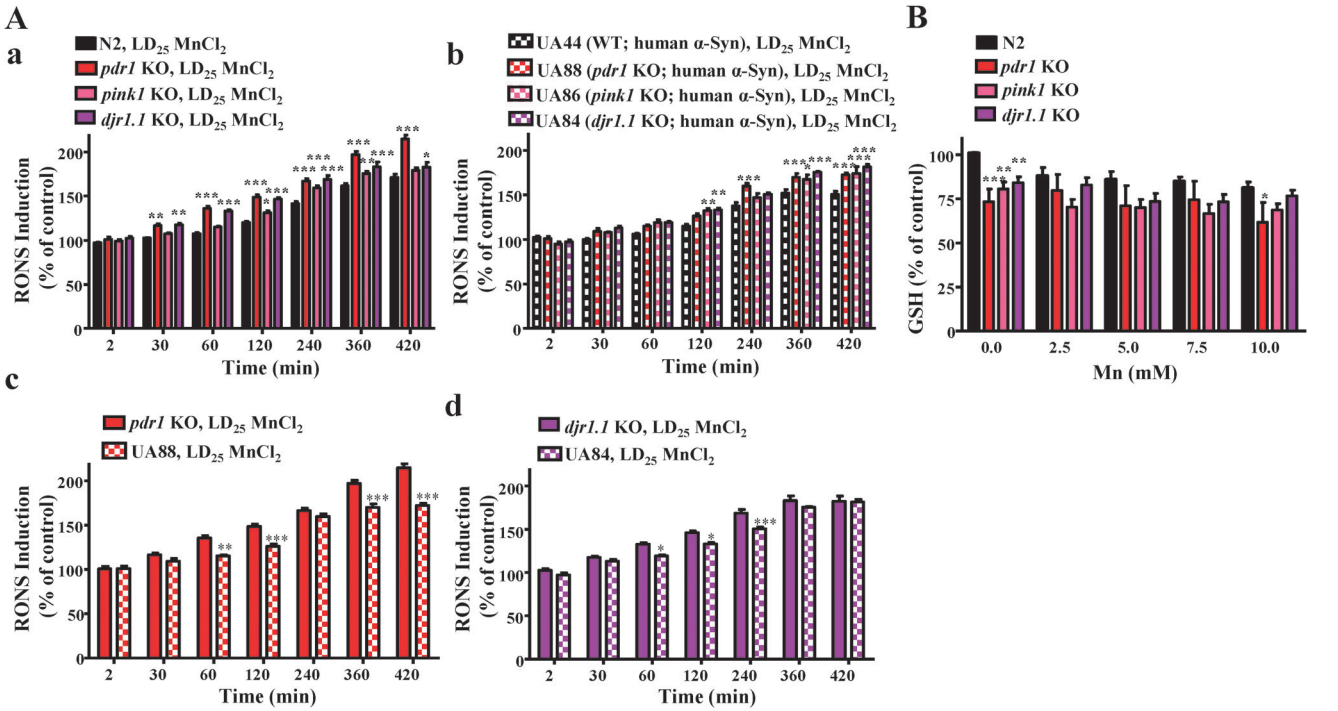

Fig. 4 Mn-induced oxidative stress is exacerbated in *pdr1* and *djr1.1* mutants, but reduced by α-Syn expression. (A) (a) Effect of $MnCl_2$ on the RONS induction in N2 (WT) and *pdr1*, *pink1* and *djr1.1* deletion mutants after 1 h dye loading and subsequent $MnCl_2$ post-treatment with their respective LD_{25} doses. (b) Effect of $MnCl_2$ on the RONS induction of UA44 (WT; human α-Syn), UA88 (*pdr1* KO; human α-Syn), UA86 (*pink1* KO; human α-Syn) and UA84 (*djr1.1* KO; human α-Syn) after 1 h dye loading and subsequent $MnCl_2$ post-treatment with their respective LD_{25} doses. (c) Comparing Mn-induced RONS induction of *pdr1* mutants and UA88 (*pdr1* KO; human α-Syn) (see B, a and B, b). (d) Comparing Mn-induced RONS induction of *djr1.1* mutants and UA84 (*djr1.1* KO; human α-Syn) (see B, a and B, b). (A) Shown are mean values (+SEM) of at least four measurements, which were normalized to the respective dye-loaded worms at the respective time-points. Statistical analysis by two-way ANOVA: (a–c) interaction $p < 0.001$, genotype $p < 0.001$, time $p < 0.001$; (d) interaction ns, genotype $p < 0.001$, time $p < 0.001$. (B) Total glutathione level of N2 (WT) and *pdr1*, *pink1* and *djr1.1* deletion mutants following 30 min exposure with increasing concentrations of $MnCl_2$. Data are expressed as means + SEM from at least five independent experiments. Statistical analysis by two-way ANOVA: interaction ns, genotype $p < 0.001$, concentration $p < 0.01$. (A–C) $p < 0.001$. ***$p < 0.001$, **$p < 0.01$, *$p < 0.05$. KO = deletion mutants; ns = not significant.

Decreased *dat-1* expression in *djr1.1* deletion mutants

Since previous studies supported the role of extracellular dopamine in exacerbating Mn toxicity,[39] we further investigated possible interactions between α-Syn and the dopamine transporter (DAT), the protein responsible for synaptic DA clearance. Recent evidence points to α-Syn-mediated modulation of DAT[47] as a potential mechanism for the selectivity towards DAergic neurodegeneration in PD. Using Real Time RT PCR, we show that *pdr1* mutants have inherently higher *dat-1* mRNA levels, whereas the expression is reduced in both Mn treated and untreated *djr1.1* mutants compared to WT worms (Fig. 6). *pink1* mutants were indistinguishable from the WT worms with respect to DA neurodegeneration and *dat-1* mRNA levels (data not shown).

Discussion

The specific interactions between environmental factors and various genetic deletions associated with PD pathophysiology remain poorly understood. In the present study, the invertebrate *C. elegans* model was used to examine the effects of acute Mn exposure on DAergic neurotoxicity in the background of three PD-associated genes (*pdr1*/*parkin*, *pink1* and *djr1.1*/*dj1*) in the absence or the presence of WT human α-Syn. The ease in genetic manipulation and breeding of nematodes allowed for the quick generation and assessment of crosses needed to evaluate DAergic neurodegeneration. Moreover, this model system allows for an alternative approach to otherwise time-consuming and costly vertebrate models that contain intricate nervous systems, hindering more rapid investigations into neurodegenerative mechanisms.

Regarding the Mn-induced lethality in the present study, *pdr1* mutants showed the highest sensitivity to acute Mn exposure. Interestingly, vulnerability of the WT worms to acute $MnCl_2$ exposure has changed since our previously published paper,[39] which may be due to the current use of $MnCl_2$ with a higher purity of >99.995%. Thus, new curves were generated. Based on the different dose–response curves of the WT worms and the deletion mutants following acute Mn exposure, we examined whether they showed a differential Mn accumulation profile compared to WT worms. Interestingly, both *pdr1* and *djr1.1* mutants displayed significantly enhanced intraworm Mn accumulation, as shown by ICP-MS/MS. Mn accumulation

Published on 12 December 2013. Downloaded on 30/01/2014 17:07:09.

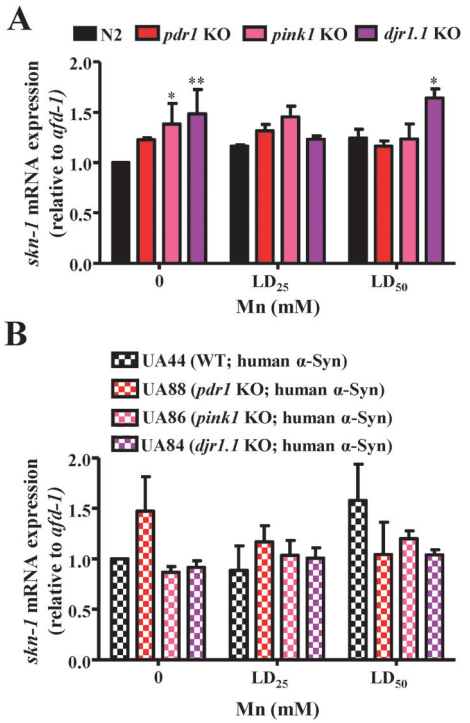

Fig. 5 Increased *skn-1* mRNA expression in *djr1.1* and *pink1* mutants. *skn-1* expression after acute treatment with $MnCl_2$. Relative gene expression was determined by qRT-PCR. (A) N2 (WT) and *pdr1*, *pink1* and *djr1.1* deletion mutants were treated at L1 stage for 30 min with $MnCl_2$ at the respective LD_{25} and LD_{50} doses. (B) UA44 (WT; human α-Syn), UA88 (*pdr1* KO; human α-Syn), UA86 (*pink1* KO; human α-Syn) and UA84 (*djr1.1* KO; human α-Syn) were treated at the L1 stage for 30 min with $MnCl_2$ at the respective LD_{25} and LD_{50} doses. (A, B) Shown are mean values ± SEM of four independent experiments in duplicates normalized to the untreated wildtype and relative to *afd-1*/*β-actin* mRNA. Statistical analysis by two-way ANOVA: (A) interaction ns, genotype $p < 0.01$, concentration; (B) interaction ns, genotype ns, concentration ns. $^{**}p < 0.01$, $^{*}p < 0.05$ *versus* respective wildtype worms. KO = deletion mutants; ns = not significant.

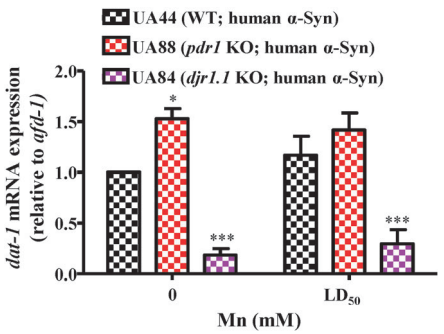

Fig. 6 Decreased *dat-1* expression in *djr1.1* deletion mutants. *dat-1* mRNA expression after acute treatment with $MnCl_2$. Relative gene expression was determined by qRT-PCR. UA44 (WT; human α-Syn), UA88 (*pdr1* KO; human α-Syn)) and UA84 (*djr1.1* KO; human α-Syn) were treated at the L1 stage for 30 min with $MnCl_2$ at the respective LD_{50}. Data are expressed as means + SEM from at least four independent experiments in duplicate normalized to the untreated wildtype and relative to *afd-1*/*β-actin* mRNA. Statistical analysis by two-way ANOVA: interaction ns, genotype $p < 0.001$, concentration ns. $^{***}p < 0.001$, $^{*}p < 0.05$ *versus* respective wildtype worms. KO = deletion mutants; ns = significant.

inside the worms (and not just a measurement of metals bound to the outer worm cuticle) was also corroborated by the novel and optimized utilization of LA-ICP-MS.[48]

Our laboratory has recently identified a network of Mn transporter genes responsible for controlling Mn homeostasis in worms. The *smf1-3* genes are orthologues for the mammalian divalent metal transporter 1 (DMT1), with SMF-3 serving as the primary Mn uptake transporter in *C. elegans*.[49] Interestingly, evidence has pointed to a parkin-mediated regulation of DMT1 levels *via* ubiquitination *in vitro*.[50] As the *pdr1* gene shows conservation of its ubiquitin ligase activity in nematodes, it is plausible that the loss of *pdr1* enhanced Mn uptake due to the loss of transporter regulation. This interaction would be interesting to examine in this model system, as the *C. elegans* genome does not have nearly as many E3 ubiquitin ligases as the human genome,[51] reducing the amount of compensatory mechanisms that may be possible in vertebrate knockout models.

Furthermore, previous evidence in *Drosophila melanogaster* has shown an increased lifespan in *parkin*-null flies upon exposure to metal chelators compared to controls, indicating a heightened sensitivity to endogenous copper (Cu^{2+}) and iron (Fe^{2+}) levels.[52] This interaction was further supported by evidence showing a reduction of the *parkin* null phenotype by overexpression of a metal transcription factor (MTF-1).[53] However, previous *C. elegans* studies in *pdr1* mutants found no increased sensitivity upon exposure to Fe^{2+} and Cu^{2+}.[54] Our current findings of enhanced intraworm Mn accumulation corroborate a distinctive connection between parkin and metal homeostasis that may be Mn-specific, as we have also previously found that the same *pdr1* mutants do not show significantly increased methylmercury (MeHg) accumulation compared to WT animals.[55]

Due to the close relationship between parkin and DJ1-associated pathways, it is possible that they may be directly regulating each other. New evidence suggests a novel role for DJ1 in reducing metal-induced cytotoxicity by directly binding metals *in vitro*. While this study found a weaker binding affinity for Mn compared to Cu^{2+} and mercury (Hg^{2+}),[56] the alterations in Mn homeostasis in the worms may result in subsequent intracellular dyshomeostasis of other metals that DJ1 would typically bind to. Therefore, it is feasible that the enhancement in Mn accumulation in *djr1.1* mutants could be due to the lack of metal binding in these animals. Notably, both *pdr1* and *djr1.1* mutants showed an analogous increase in Mn accumulation, yet they possessed differential neurodegeneration profiles. Parkin has recently been shown to downregulate DJ1 protein and mRNA levels,[57] with *parkin* knockout mice showing increased DJ1 protein levels upon proteasomal inhibition.[58] The loss of parkin (*pdr1* in our case) itself may be sufficient to cause proteasomal impairment from increased oxidative stress and abnormal accumulation of misfolded proteins. Moreover, increased expression of *djr1.1* in the background of *pdr1* loss might ameliorate overall neurotoxicity in these animals.

While manganism is distinctive from PD in terms of the initial site of metal accumulation and toxicity (globus pallidus),

 This journal is © The Royal Society of Chemistry 2014

Published on 12 December 2013. Downloaded on 30/01/2014 17:07:09.

both medical conditions implicate enhanced oxidative damage. In the absence of genetic alterations, Mn itself can cause mitochondrial damage by inhibiting complex I and II of the electron transport chain (ETC) and oxidative phosphorylation.[59] Mn can also increase isoprostane (lipid peroxidation marker) generation[60] and decrease ATP levels in a dose-dependent manner, resulting in increased neurodegeneration.[44] The increased intraworm Mn concentrations may also influence iron (Fe) concentrations, another heavy metal that competes with Mn for transport *via* DMT1 and the transferrin receptor (TfR).[61] Furthermore, iron has been implicated in PD by promoting oxidative damage *via* the Fenton reaction or altering oxidative response pathways.[62] Mn has also been shown to exacerbate DA oxidation to produce damaging, reactive DA intermediates.[63] The combination of Mn's own oxidative potential and enhancement of DA oxidation, represent a plausible mechanism for its selectivity towards DAergic neurodegeneration, as previously corroborated in *C. elegans*.[39]

The marked increase in baseline RONS induction in the *pdr1* mutants was striking; however, this is not surprising, as parkin's significant role in mediating mitophagy warrants impaired mitochondrial integrity in its absence.[17a,64] The similarly elevated basal RONS levels in the *djr1.1* mutants do not quite reach the level of the *pdr1* mutants. As noted earlier, several studies have affirmed DJ1's role as an oxidative stress sensor, indicating that loss of DJ1 would inherently result in increased RONS production.[20] We posit that this inherently enhanced level of RONS induction accounts for an attenuated response upon acute Mn exposure, as these mutants exhibit a ceiling effect to the already-high baseline RONS levels. Given its role in recruiting parkin to damaged mitochondria, it was somewhat unexpected that *pink1* mutants only showed a slightly enhanced RONS induction compared to WT worms. However, the presence of DJ1 in *Drosophila* is capable of reducing mitochondrial deficits in the background of *pink1*, but not *parkin* loss.[25] This could account for the lack of an oxidative stress phenotype in the *pink1* mutants, as well as the fact that these mutants did not take up as much Mn as the *pdr1* and *djr1.1* mutants.

While a trend was apparent towards a dose-dependent effect of Mn on GSH depletion in WT animals, the deletion mutants show no significant change with treatment. In particular, the baseline reduction in GSH levels in all deletion mutants suggests an inherently impaired ability to adapt to stressful stimuli, such as acute Mn exposure. In *pdr1* mutants, this may also relate to the inherently high levels of RONS production, as they show the lowest basal total GSH levels. Moreover, it has been shown that knocking down *pink1* in human neurons results in GSH reduction.[45] Similarly, DJ1 expression promotes upregulation of glutathione synthesis,[65] which corresponds with the finding in *djr1.1* mutants, showing decreased GSH levels. Taken together, our data support a mechanism of neurotoxicity through compromised clearance of Mn-damaged mitochondria due to the loss of an intact parkin/PINK1/DJ1 pathway, resulting in heightened RONS production that cannot be inherently combated due to basal GSH deficiencies in the mutants.

The observed increase in RONS induction and basal GSH depletion in mutants showing enhanced Mn accumulation (*pdr1* and *djr1.1*) warranted further examination into whether these animals also have alterations in *skn-1* expression, the worm orthologue for *nrf2*. Nuclear factor erythroid 2-related factor 2, or Nrf2, is a transcription factor that promotes the upregulation of antioxidant genes upon oxidative-stress-induced translocation from the cytoplasm to the nucleus.[66] Previous work has found *skn-1* mutants to be vulnerable to oxidative stress.[67] While not significant, *pdr1* mutants showed a trend for increased *skn-1* mRNA expression, which was consistent with increased Nrf2 activity found in an induced pluripotent stem cell (iPSC) study in patients harboring *parkin* mutations.[68] Moreover, contrary to DJ1 acting as an Nrf2 stabilizer,[69] we found significantly increased *skn-1* mRNA expression in the *djr1.1* mutants. While we did not expect this increase, there may be a compensatory mechanism in these animals to counteract the basal GSH depletion that would otherwise protect against RONS production by upregulating *skn-1*-mediated antioxidant gene transcription.

Additionally, the enhanced oxidative stress of the *pdr1* and *djr1.1* mutants occurs in the absence of Mn-induced DAergic neurodegeneration. Similarly, the lack of subacute Mn-induced changes in the basal ganglia has been previously shown in primates.[70] Thus, the findings in this study corroborate that Mn is even more relevant in exacerbating genetic risk for PD. In a previously published study from our group, Mn showed a selective effect on dopaminergic neurons in WT worms 24 hours post-treatment.[39] This is not in conflict with the current study, given the use of a new, objective scoring for the degenerated architecture of CEP neurons, along with differing Mn doses newly generated from the survival curves.

Although α-Syn is known to be involved in the pathogenesis of PD, its role in both neuroprotection and neurodegeneration is controversial. Mutated forms of α-Syn, (A30P, E46K, A53T) have been reported to be neurotoxic, while WT α-Syn has been implicated in neuroprotection.[71] α-Syn is a neuronal protein in vertebrates that is ubiquitously expressed at high levels in all brain regions,[72] but it is not expressed in *C. elegans*. Therefore, worms expressing human WT α-Syn were utilized to address the role of α-Syn in the mutated background of *pdr1*, *pink1* and *djr1.1* with respect to Mn homeostasis and oxidative stress.

There is increasing evidence that α-Syn interacts with metal ions, thereby affecting their homeostasis. Initial studies of the potential to bind metals came from the ability of certain metals to catalyze α-Syn aggregation.[73] Overall, two major types of interactions between metals and α-Syn have been reported. In addition to non-specific sites of electrostatic interactions, the C-terminus contains a ^{119}DPDNEA motif binding site, suggesting that metal binding is driven by both electrostatic interactions and the residual structure of the α-Syn C-terminus. The C-terminal low-affinity sites have been reported to interact with different metal ions, with copper (Cu) and Fe most intensively studied.[74] Although the majority of metal ions interact with α-Syn with low affinity, the protein possesses high affinity to Cu^{2+} and Fe^{3+} at the N-terminal region. Modifications by redox-active

Published on 12 December 2013. Downloaded on 30/01/2014 17:07:09.

metal ions may be relevant for the aggregation properties of α-Syn.[75] A co-incubation of α-Syn with Mn^{2+} has been reported to induce partial folding of the protein and serve as an effective promoter of α-Syn aggregation.[76]

In addition to its metal binding capacity, the role of α-Syn as a cellular ferrireductase has been recently identified, providing further evidence towards the multiple roles of α-Syn in metal homeostasis.[77] One very important outcome of the present work is the novel role of α-Syn in altering Mn accumulation in the background of mutated *pdr1* and *djr1.1* worms, which may be partially due to an endogenous metal binding capacity. Even as α-Syn was only expressed in the DAergic neurons of the worms, the global alterations in Mn homeostasis were drastic; secretion of α-Syn into other regions cannot be excluded.[78] In fact, an environmental toxin (*i.e.* rotenone) has been shown to promote the release of α-Syn from enteric neurons.[79]

In terms of the role of α-Syn in modulating oxidative stress responses, the loss of *pdr1* or *djr1.1* in α-Syn-expressing worms resulted in reduced Mn-induced RONS production, compared to worms containing the genetic deletion alone. This effect was due to the reduced Mn accumulation in the presence of α-Syn in both *pdr1* and *djr1.1* deletion backgrounds. Additionally, attenuated oxidative stress, in accordance with the neuroprotective role of α-Syn, has been shown in cells expressing WT α-Syn, where protection against rotenone and maneb toxicity was conferred by preservation of mitochondrial function.[71b] Additionally, WT α-Syn-expressing cells also showed the ability to attenuate decreased intracellular GSH levels upon serum deprivation.[80] The results in the current study support the literature in finding a neuroprotective role of wildtype α-Syn against oxidative stress.

Since one function of α-Syn is the modulation of the dopamine transporter (DAT) and loss of *dat-1* is detrimental to worm survival following acute Mn exposure, dat-1 expression was investigated. This transporter (DAT-1 in *C. elegans*) is involved in synaptic neurotransmitter clearance, and especially responsible for DA reuptake to remove excessive extracellular DA concentrations.[81] Inhibition of DAT leads to high extracellular DA levels.[82] In *C. elegans*, we have already shown that upon Mn exposure, loss of *dat-1* increases Mn-induced lethality compared to WT worms, with extracellular DA exacerbating Mn-induced oxidative stress, lifespan reduction and DAergic neurodegeneration.[39] While *pdr1* mutants showed inherently higher *dat-1* mRNA levels, the down-regulation of *dat-1* mRNA in the djr1.1 mutants suggests a reduced synaptic DA clearance. This might be due to the increased DAergic neurodegeneration of the α-Syn-containing *djr1.1* deletion mutants compared to the α-Syn-containing *pdr1* deletion mutants. The increased *dat-1* levels would suggest higher extracellular DA levels in the *djr1.1* mutants as a potential mechanism behind the enhanced neurodegeneration. Taken together, these findings support the role of extracellular DA in exacerbating Mn neurotoxicity.

Conclusions

The genetically amenable *C. elegans* model system was utilized to examine the neuroprotective or neurotoxic role of α-Syn in mediating Mn neurotoxicity in the background of loss in the PD-associated genes *pdr1*, *pink1* and *djr1.1*. For the first time, the current study provides evidence for a neuroprotective role of WT α-Syn against Mn accumulation and Mn-induced oxidative stress in the background of *pdr1* and *djr1.1* loss.

Acknowledgements

This work was funded by the Center in Molecular Toxicology NIH grant P30 ES00267, R01 ES10563, the training program in Environmental Toxicology grant T32 ES007028, the Josef Schormüller Award and the DFG (BO 4103/1-1). We would also like to thank the Blakely laboratory (Vanderbilt University Medical Center) for strains and sharing resources. Lastly, we would like to thank Drs Bill Valentine and Keith Erikson for sharing resources and scientific communications.

References

1 ATSDR, Toxicological profile for manganese (Draft for Public Comment), U.S. Department of Health and Human Services, Public Service, 2008.
2 A. J. Lees, J. Hardy and T. Revesz, Parkinson's disease, *Lancet*, 2009, **373**, 2055–2066, DOI: 10.1016/S0140-6736(09)60492-X.
3 T. M. Dawson, H. S. Ko and V. L. Dawson, Genetic animal models of Parkinson's disease, *Neuron*, 2010, **66**, 646–661, DOI: 10.1016/j.neuron.2010.04.034.
4 T. Kitada, S. Asakawa, N. Hattori, H. Matsumine, Y. Yamamura, S. Minoshima, M. Yokochi, Y. Mizuno and N. Shimizu, Mutations in the parkin gene cause autosomal recessive juvenile parkinsonism, *Nature*, 1998, **392**, 605–608, DOI: 10.1038/33416.
5 Y. Zhang, J. Gao, K. K. Chung, H. Huang, V. L. Dawson and T. M. Dawson, Parkin functions as an E2-dependent ubiquitin-protein ligase and promotes the degradation of the synaptic vesicle-associated protein, CDCrel-1, *Proc. Natl. Acad. Sci. U. S. A.*, 2000, **97**, 13354–13359, DOI: 10.1073/pnas240347797.
6 S. R. Sriram, X. Li, H. S. Ko, K. K. Chung, E. Wong, K. L. Lim, V. L. Dawson and T. M. Dawson, Familial-associated mutations differentially disrupt the solubility, localization, binding and ubiquitination properties of parkin, *Hum. Mol. Genet.*, 2005, **14**, 2571–2586, DOI: 10.1093/hmg/ddi292.
7 T. K. Sang, H. Y. Chang, G. M. Lawless, A. Ratnaparkhi, L. Mee, L. C. Ackerson, N. T. Maidment, D. E. Krantz and G. R. Jackson, A Drosophila model of mutant human parkin-induced toxicity demonstrates selective loss of dopaminergic neurons and dependence on cellular dopamine, *J. Neurosci.*, 2007, **27**, 981–992, DOI: 10.1523/JNEUROSCI.4810-06.2007.
8 M. S. Goldberg, S. M. Fleming, J. J. Palacino, C. Cepeda, H. A. Lam, A. Bhatnagar, E. G. Meloni, N. Wu, L. C. Ackerson, G. J. Klapstein, M. Gajendiran, B. L. Roth, M. F. Chesselet, N. T. Maidment, M. S. Levine and J. Shen, Parkin-deficient mice exhibit nigrostriatal deficits but not loss of dopaminergic neurons, *J. Biol. Chem.*, 2003, **278**, 43628–43635, DOI: 10.1074/jbc.M308947200.

 This journal is © The Royal Society of Chemistry 2014

Published on 12 December 2013. Downloaded on 30/01/2014 17:07:09.

9 (*a*) M. Unoki and Y. Nakamura, Growth-suppressive effects of BPOZ and EGR2, two genes involved in the PTEN signaling pathway, *Oncogene*, 2001, **20**, 4457–4465, DOI: 10.1038/sj.onc.1204608; (*b*) M. Jendrach, S. Gispert, F. Ricciardi, M. Klinkenberg, R. Schemm and G. Auburger, The mitochondrial kinase PINK1, stress response and Parkinson's disease, *J. Bioenerg. Biomembr.*, 2009, **41**, 481–486, DOI: 10.1007/s10863-009-9256-0.

10 E. M. Valente, P. M. Abou-Sleiman, V. Caputo, M. M. Muqit, K. Harvey, S. Gispert, Z. Ali, D. Del Turco, A. R. Bentivoglio, D. G. Healy, A. Albanese, R. Nussbaum, R. Gonzalez-Maldonado, T. Deller, S. Salvi, P. Cortelli, W. P. Gilks, D. S. Latchman, R. J. Harvey, B. Dallapiccola, G. Auburger and N. W. Wood, Hereditary early-onset Parkinson's disease caused by mutations in PINK1, *Science*, 2004, **304**, 1158–1160, DOI: 10.1126/science.1096284.

11 C. H. Sim, D. S. Lio, S. S. Mok, C. L. Masters, A. F. Hill, J. G. Culvenor and H. C. Cheng, C-terminal truncation and Parkinson's disease-associated mutations down-regulate the protein serine/threonine kinase activity of PTEN-induced kinase-1, *Hum. Mol. Genet.*, 2006, **15**, 3251–3262, DOI: 10.1093/hmg/ddl398.

12 Y. Yang, Y. Ouyang, L. Yang, M. F. Beal, A. McQuibban, H. Vogel and B. Lu, Pink1 regulates mitochondrial dynamics through interaction with the fission/fusion machinery, *Proc. Natl. Acad. Sci. U. S. A.*, 2008, **105**, 7070–7075, DOI: 10.1073/pnas0711845105.

13 H. Plun-Favreau, K. Klupsch, N. Moisoi, S. Gandhi, S. Kjaer, D. Frith, K. Harvey, E. Deas, R. J. Harvey, N. McDonald, N. W. Wood, L. M. Martins and J. Downward, The mitochondrial protease HtrA2 is regulated by Parkinson's disease-associated kinase PINK1, *Nat. Cell Biol.*, 2007, **9**, 1243–1252, DOI: 10.1038/ncb1644.

14 A. Petit, T. Kawarai, E. Paitel, N. Sanjo, M. Maj, M. Scheid, F. Chen, Y. Gu, H. Hasegawa, S. Salehi-Rad, L. Wang, E. Rogaeva, P. Fraser, B. Robinson, P. St George-Hyslop and A. Tandon, Wild-type PINK1 prevents basal and induced neuronal apoptosis, a protective effect abrogated by Parkinson disease-related mutations, *J. Biol. Chem.*, 2005, **280**, 34025–34032, DOI: 10.1074/jbc.M505143200.

15 S. Gandhi, A. Vaarmann, Z. Yao, M. R. Duchen, N. W. Wood and A. Y. Abramov, Dopamine induced neurodegeneration in a PINK1 model of Parkinson's disease, *PLoS One*, 2012, **7**, e37564, DOI: 10.1371/journal.pone.0037564.

16 T. Kitada, A. Pisani, D. R. Porter, H. Yamaguchi, A. Tscherter, G. Martella, P. Bonsi, C. Zhang, E. N. Pothos and J. Shen, Impaired dopamine release and synaptic plasticity in the striatum of PINK1-deficient mice, *Proc. Natl. Acad. Sci. U. S. A.*, 2007, **104**, 11441–11446, DOI: 10.1073/pnas0702717104.

17 (*a*) C. Vives-Bauza, C. Zhou, Y. Huang, M. Cui, R. L. de Vries, J. Kim, J. May, M. A. Tocilescu, W. Liu, H. S. Ko, J. Magrane, D. J. Moore, V. L. Dawson, R. Grailhe, T. M. Dawson, C. Li, K. Tieu and S. Przedborski, PINK1-dependent recruitment of Parkin to mitochondria in mitophagy, *Proc. Natl. Acad. Sci. U. S. A.*, 2010, **107**, 378–383, DOI: 10.1073/pnas.0911187107; (*b*) Y. Kim, J. Park, S. Kim, S. Song, S. K. Kwon, S. H. Lee, T. Kitada, J. M. Kim and J. Chung, PINK1 controls mitochondrial localization of Parkin through direct phosphorylation, *Biochem. Biophys. Res. Commun.*, 2008, **377**, 975–980, DOI: 10.1016/j.bbrc.2008.10.104; (*c*) K. Okatsu, T. Oka, M. Iguchi, K. Imamura, H. Kosako, N. Tani, M. Kimura, E. Go, F. Koyano, M. Funayama, K. Shiba-Fukushima, S. Sato, H. Shimizu, Y. Fukunaga, H. Taniguchi, M. Komatsu, N. Hattori, K. Mihara, K. Tanaka and N. Matsuda, PINK1 autophosphorylation upon membrane potential dissipation is essential for Parkin recruitment to damaged mitochondria, *Nat. Commun.*, 2012, **3**, 1016, DOI: 10.1038/ncomms2016.

18 (*a*) Y. Chen and G. W. Dorn, 2nd, PINK1-phosphorylated mitofusin 2 is a Parkin receptor for culling damaged mitochondria, *Science*, 2013, **340**, 471–475, DOI: 10.1126/science.1231031; (*b*) Y. Sun, A. A. Vashisht, J. Tchieu, J. A. Wohlschlegel and L. Dreier, Voltage-dependent anion channels (VDACs) recruit Parkin to defective mitochondria to promote mitochondrial autophagy, *J. Biol. Chem.*, 2012, **287**, 40652–40660, DOI: 10.1074/jbc.M112.419721.

19 V. Bonifati, P. Rizzu, M. J. van Baren, O. Schaap, G. J. Breedveld, E. Krieger, M. C. Dekker, F. Squitieri, P. Ibanez, M. Joosse, J. W. van Dongen, N. Vanacore, J. C. van Swieten, A. Brice, G. Meco, C. M. van Duijn, B. A. Oostra and P. Heutink, Mutations in the DJ-1 gene associated with autosomal recessive early-onset parkinsonism, *Science*, 2003, **299**, 256–259, DOI: 10.1126/science.1077209.

20 R. M. Canet-Aviles, M. A. Wilson, D. W. Miller, R. Ahmad, C. McLendon, S. Bandyopadhyay, M. J. Baptista, D. Ringe, G. A. Petsko and M. R. Cookson, The Parkinson's disease protein DJ-1 is neuroprotective due to cysteine-sulfinic acid-driven mitochondrial localization, *Proc. Natl. Acad. Sci. U. S. A.*, 2004, **101**, 9103–9108, DOI: 10.1073/pnas0402959101.

21 X. Wang, T. G. Petrie, Y. Liu, J. Liu, H. Fujioka and X. Zhu, Parkinson's disease-associated DJ-1 mutations impair mitochondrial dynamics and cause mitochondrial dysfunction, *J. Neurochem.*, 2012, **121**, 830–839, DOI: 10.1111/j.1471-4159.2012.07734.x.

22 M. Inden, T. Taira, Y. Kitamura, T. Yanagida, D. Tsuchiya, K. Takata, D. Yanagisawa, K. Nishimura, T. Taniguchi, Y. Kiso, K. Yoshimoto, T. Agatsuma, S. Koide-Yoshida, S. M. Iguchi-Ariga, S. Shimohama and H. Ariga, PARK7 DJ-1 protects against degeneration of nigral dopaminergic neurons in Parkinson's disease rat model, *Neurobiol. Dis.*, 2006, **24**, 144–158, DOI: 10.1016/j.nbd.2006.06.004.

23 H. Xiong, D. Wang, L. Chen, Y. S. Choo, H. Ma, C. Tang, K. Xia, W. Jiang, Z. Ronai, X. Zhuang and Z. Zhang, Parkin, PINK1, and DJ-1 form a ubiquitin E3 ligase complex promoting unfolded protein degradation, *J. Clin. Invest.*, 2009, **119**, 650–660, DOI: 10.1172/JCI37617.

24 M. E. Haque, M. P. Mount, F. Safarpour, E. Abdel-Messih, S. Callaghan, C. Mazerolle, T. Kitada, R. S. Slack, V. Wallace, J. Shen, H. Anisman and D. S. Park, Inactivation of Pink1 gene *in vivo* sensitizes dopamine-producing neurons to 1-methyl-4-phenyl-1,2,3,6-tetrahydropyridine (MPTP) and can be reduced by autosomal recessive Parkinson disease

Published on 12 December 2013. Downloaded on 30/01/2014 17:07:09.

genes, Parkin or DJ-1, *J. Biol. Chem.*, 2012, **287**, 23162–23170, DOI: 10.1074/jbc.M112.346437.

25 L. Y. Hao, B. I. Giasson and N. M. Bonini, DJ-1 is critical for mitochondrial function and reduces PINK1 loss of function, *Proc. Natl. Acad. Sci. U. S. A.*, 2010, **107**, 9747–9752, DOI: 10.1073/pnas0911175107.

26 M. H. Polymeropoulos, C. Lavedan, E. Leroy, S. E. Ide, A. Dehejia, A. Dutra, B. Pike, H. Root, J. Rubenstein, R. Boyer, E. S. Stenroos, S. Chandrasekharappa, A. Athanassiadou, T. Papapetropoulos, W. G. Johnson, A. M. Lazzarini, R. C. Duvoisin, G. Di Iorio, L. I. Golbe and R. L. Nussbaum, Mutation in the alpha-synuclein gene identified in families with Parkinson's disease, *Science*, 1997, **276**, 2045–2047.

27 (*a*) L. R. Lemkau, G. Comellas, S. W. Lee, L. K. Rikardsen, W. S. Woods, J. M. George and C. M. Rienstra, Site-specific perturbations of alpha-synuclein fibril structure by the Parkinson's disease associated mutations A53T and E46K, *PLoS One*, 2013, **8**, e49750, DOI: 10.1371/journal.pone.0049750; (*b*) K. A. Conway, S. J. Lee, J. C. Rochet, T. T. Ding, R. E. Williamson and P. T. Lansbury, Jr., Acceleration of oligomerization, not fibrillization, is a shared property of both alpha-synuclein mutations linked to early-onset Parkinson's disease: implications for pathogenesis and therapy, *Proc. Natl. Acad. Sci. U. S. A.*, 2000, **97**, 571–576.

28 (*a*) D. D. Murphy, S. M. Rueter, J. Q. Trojanowski and V. M. Lee, Synucleins are developmentally expressed, and alpha-synuclein regulates the size of the presynaptic vesicular pool in primary hippocampal neurons, *J. Neurosci.*, 2000, **20**, 3214–3220; (*b*) J. Diao, J. Burre, S. Vivona, D. J. Cipriano, M. Sharma, M. Kyoung, T. C. Sudhof and A. T. Brunger, Native alpha-synuclein induces clustering of synaptic-vesicle mimics via binding to phospholipids and synaptobrevin-2/VAMP2, *eLife*, 2013, **2**, e00592, DOI: 10.7554/eLife.00592.

29 M. N. Gaugler, O. Genc, W. Bobela, S. Mohanna, M. T. Ardah, O. M. El-Agnaf, M. Cantoni, J. C. Bensadoun, R. Schneggenburger, G. W. Knott, P. Aebischer and B. L. Schneider, Nigrostriatal overabundance of alpha-synuclein leads to decreased vesicle density and deficits in dopamine release that correlate with reduced motor activity, *Acta Neuropathol.*, 2012, **123**, 653–669, DOI: 10.1007/s00401-012-0963-y.

30 R. G. Perez, J. C. Waymire, E. Lin, J. J. Liu, F. Guo and M. J. Zigmond, A role for alpha-synuclein in the regulation of dopamine biosynthesis, *J. Neurosci.*, 2002, **22**, 3090–3099.

31 T. N. Alerte, A. A. Akinfolarin, E. E. Friedrich, S. A. Mader, C. S. Hong and R. G. Perez, Alpha-synuclein aggregation alters tyrosine hydroxylase phosphorylation and immunoreactivity: lessons from viral transduction of knockout mice, *Neurosci. Lett.*, 2008, **435**, 24–29, DOI: 10.1016/j.neulet.2008.02.014.

32 J. L. Aschner and M. Aschner, Nutritional aspects of manganese homeostasis, *Mol. Aspects Med.*, 2005, **26**, 353–362, DOI: 10.1016/j.mam.2005.07.003.

33 (*a*) T. R. Guilarte, Manganese and Parkinson's disease: a critical review and new findings, *Environ. Health Perspect.*, 2010, **118**, 1071–1080, DOI: 10.1289/ehp.0901748; (*b*) M. Aschner, K. M. Erikson, E. Herrero Hernandez and R. Tjalkens, Manganese and its role in Parkinson's disease: from transport to neuropathology, *NeuroMol. Med.*, 2009, **11**, 252–266, DOI: 10.1007/s12017-009-8083-0; (*c*) B. A. Racette, Manganism in the 21st century: The Hanninen lecture, *Neurotoxicology*, 2013, DOI: 10.1016/j.neuro.2013.09.007; (*d*) K. Tuschl, P. B. Mills and P. T. Clayton, Manganese and the brain, *Int. Rev. Neurobiol.*, 2013, **110**, 277–312, DOI: 10.1016/B978-0-12-410502-7.00013-2.

34 N. C. Burton and T. R. Guilarte, Manganese neurotoxicity: lessons learned from longitudinal studies in nonhuman primates, *Environ. Health Perspect.*, 2009, **117**, 325–332, DOI: 10.1289/ehp.0800035.

35 K. Sriram, G. X. Lin, A. M. Jefferson, J. R. Roberts, O. Wirth, Y. Hayashi, K. M. Krajnak, J. M. Soukup, A. J. Ghio, S. H. Reynolds, V. Castranova, A. E. Munson and J. M. Antonini, Mitochondrial dysfunction and loss of Parkinson's disease-linked proteins contribute to neurotoxicity of manganese-containing welding fumes, *FASEB J.*, 2010, **24**, 4989–5002, DOI: 10.1096/fj.10-163964.

36 Y. Higashi, M. Asanuma, I. Miyazaki, N. Hattori, Y. Mizuno and N. Ogawa, Parkin attenuates manganese-induced dopaminergic cell death, *J. Neurochem.*, 2004, **89**, 1490–1497, DOI: 10.1111/j.1471-4159.2004.02445.x.

37 S. Brenner, The genetics of Caenorhabditis elegans, *Genetics*, 1974, **77**, 71–94.

38 P. W. J. M. Boumans, *Inductively Coupled Plasma Emission Spectroscopy, Part 2: Applications And Fundamentals*, John Wiley & Sons, New York, 1987.

39 A. Benedetto, C. Au, D. S. Avila, D. Milatovic and M. Aschner, Extracellular dopamine potentiates mn-induced oxidative stress, lifespan reduction, and dopaminergic neurodegeneration in a BLI-3-dependent manner in Caenorhabditis elegans, *PLoS Genet.*, 2010, **6**, 18, DOI: 10.1371/journal.pgen.1001084.

40 (*a*) I. Rahman, A. Kode and S. K. Biswas, Assay for quantitative determination of glutathione and glutathione disulfide levels using enzymatic recycling method, *Nat. Protoc.*, 2006, **1**, 3159–3165, DOI: 10.1038/nprot.2006.378; (*b*) S. W. Caito, W. M. Valentine and M. Aschner, Dopaminergic neurotoxicity of S-ethyl N,N-dipropylthiocarbamate (EPTC), molinate, and S-methyl-N,N-diethylthiocarbamate (MeDETC) in Caenorhabditis elegans, *J. Neurochem.*, 2013, **127**, 837–851, DOI: 10.1111/jnc.12349.

41 K. J. Livak and T. D. Schmittgen, Analysis of relative gene expression data using real-time quantitative PCR and the 2(-Delta Delta C(T)) Method, *Methods*, 2001, **25**, 402–408, DOI: 10.1006/meth.2001.1262.

42 (*a*) WormBase.org, http://www.wormbase.org/species/c_elegans /gene/WBGene00015184#0-9d6-3; (*b*) J. Y. Lee, J. Song, K. Kwon, S. Jang, C. Kim, K. Baek, J. Kim and C. Park, Human DJ-1 and its homologs are novel glyoxalases, *Hum. Mol. Genet.*, 2012, **21**, 3215–3225, DOI: 10.1093/hmg/dds155.

43 L. D. Jayanthi, S. Apparsundaram, M. D. Malone, E. Ward, D. M. Miller, M. Eppler and R. D. Blakely, The Caenorhabditis elegans gene T23G5.5 encodes an antidepressant- and

Published on 12 December 2013. Downloaded on 30/01/2014 17:07:09.

cocaine-sensitive dopamine transporter, *Mol. Pharmacol.*, 1998, **54**, 601–609.

44 D. Milatovic, S. Zaja-Milatovic, R. C. Gupta, Y. Yu and M. Aschner, Oxidative damage and neurodegeneration in manganese-induced neurotoxicity, *Toxicol. Appl. Pharmacol.*, 2009, **240**, 219–225, DOI: 10.1016/j.taap.2009.07.004.

45 M. M. Wilhelmus, P. G. Nijland, B. Drukarch, H. E. de Vries and J. van Horssen, Involvement and interplay of Parkin, PINK1, and DJ1 in neurodegenerative and neuroinflammatory disorders, *Free Radical Biol. Med.*, 2012, **53**, 983–992, DOI: 10.1016/j.freeradbiomed.2012.05.040.

46 R. P. Oliveira, J. Porter Abate, K. Dilks, J. Landis, J. Ashraf, C. T. Murphy and T. K. Blackwell, Condition-adapted stress and longevity gene regulation by Caenorhabditis elegans SKN-1/Nrf, *Aging Cell*, 2009, **8**, 524–541, DOI: 10.1111/j.1474-9726.2009.00501.x.

47 J. Swant, J. S. Goodwin, A. North, A. A. Ali, J. Gamble-George, S. Chirwa and H. Khoshbouei, alpha-Synuclein stimulates a dopamine transporter-dependent chloride current and modulates the activity of the transporter, *J. Biol. Chem.*, 2011, **286**, 43933–43943, DOI: 10.1074/jbc.M111.241232.

48 J. S. Becker, M. V. Zoriy, C. Pickhardt, N. Palomero-Gallagher and K. Zilles, Imaging of copper, zinc, and other elements in thin section of human brain samples (hippocampus) by laser ablation inductively coupled plasma mass spectrometry, *Anal. Chem.*, 2005, **77**, 3208–3216, DOI: 10.1021/ac040184q.

49 C. Au, A. Benedetto, J. Anderson, A. Labrousse, K. Erikson, J. J. Ewbank and M. Aschner, SMF-1, SMF-2 and SMF-3 DMT1 orthologues regulate and are regulated differentially by manganese levels in C. elegans, *PLoS One*, 2009, **4**, e7792, DOI: 10.1371/journal.pone.0007792.

50 J. A. Roth, S. Singleton, J. Feng, M. Garrick and P. N. Paradkar, Parkin regulates metal transport via proteasomal degradation of the 1B isoforms of divalent metal transporter 1, *J. Neurochem.*, 2010, **113**, 454–464, DOI: 10.1111/j.1471-4159.2010.06607.x.

51 E. T. Kipreos, Ubiquitin-mediated pathways in C. elegans, *WormBook: the online review of C. elegans biology*, 2005, vol. 1, p. 24, 10.1895/wormbook.1.36.1.

52 N. Saini, S. Oelhafen, H. Hua, O. Georgiev, W. Schaffner and H. Bueler, Extended lifespan of Drosophila parkin mutants through sequestration of redox-active metals and enhancement of anti-oxidative pathways, *Neurobiol. Dis.*, 2010, **40**, 82–92, DOI: 10.1016/j.nbd.2010.05.011.

53 N. Saini, O. Georgiev and W. Schaffner, The parkin mutant phenotype in the fly is largely reduced by metal-responsive transcription factor (MTF-1), *Mol. Cell. Biol.*, 2011, **31**, 2151–2161, DOI: 10.1128/MCB.05207-11.

54 R. Ved, S. Saha, B. Westlund, C. Perier, L. Burnam, A. Sluder, M. Hoener, C. M. Rodrigues, A. Alfonso, C. Steer, L. Liu, S. Przedborski and B. Wolozin, Similar patterns of mitochondrial vulnerability and reduction induced by genetic modification of alpha-synuclein, parkin, and DJ-1 in Caenorhabditis elegans, *J. Biol. Chem.*, 2005, **280**, 42655–42668, DOI: 10.1074/jbc.M505910200.

55 E. J. Martinez-Finley, S. Chakraborty, J. C. Slaughter and M. Aschner, Early-Life Exposure to Methylmercury in Wild-type and pdr-1/parkin Knockout C. elegans, *Neurochem. Res.*, 2013, **38**, 1543–1552, DOI: 10.1007/s11064-013-1054-8.

56 B. Bjorkblom, A. Adilbayeva, J. Maple-Grodem, D. Piston, M. Okvist, X. M. Xu, C. Brede, J. P. Larsen and S. G. Moller, Parkinson Disease Protein DJ-1 Binds Metals and Protects against Metal-induced Cytotoxicity, *J. Biol. Chem.*, 2013, **288**, 22809–22820, DOI: 10.1074/jbc.M113.482091.

57 E. Duplan, E. Giaime, J. Viotti, J. Sevalle, O. Corti, A. Brice, H. Ariga, L. Qi, F. Checler and C. Alves da Costa, ER-stress-associated functional link between Parkin and DJ-1 via a transcriptional cascade involving the tumor suppressor p53 and the spliced X-box binding protein XBP-1, *J. Cell Sci.*, 2013, **126**, 2124–2133, DOI: 10.1242/jcs.127340.

58 M. J. Casarejos, R. M. Solano, J. A. Rodriguez-Navarro, A. Gomez, J. Perucho, J. G. Castano, J. Garcia de Yebenes and M. A. Mena, Parkin deficiency increases the resistance of midbrain neurons and glia to mild proteasome inhibition: the role of autophagy and glutathione homeostasis, *J. Neurochem.*, 2009, **110**, 1523–1537, DOI: 10.1111/j.1471-4159.2009.06248.x.

59 (*a*) C. E. Gavin, K. K. Gunter and T. E. Gunter, Mn^{2+} sequestration by mitochondria and inhibition of oxidative phosphorylation, *Toxicol. Appl. Pharmacol.*, 1992, **115**, 1–5; (*b*) Y. Liu, D. S. Barber, P. Zhang and B. Liu, Complex II of the mitochondrial respiratory chain is the key mediator of divalent manganese-induced hydrogen peroxide production in microglia, *Toxicol. Sci.*, 2013, **132**, 298–306, DOI: 10.1093/toxsci/kfs344.

60 F. M. Cordova, A. S. Aguiar, Jr., T. V. Peres, M. W. Lopes, F. M. Goncalves, D. Z. Pedro, S. C. Lopes, C. Pilati, R. D. Prediger, M. Farina, K. M. Erikson, M. Aschner and R. B. Leal, Manganese-exposed developing rats display motor deficits and striatal oxidative stress that are reversed by Trolox, *Arch. Toxicol.*, 2013, **87**, 1231–1244, DOI: 10.1007/s00204-013-1017-5.

61 K. M. Erikson, T. Syversen, J. L. Aschner and M. Aschner, Interactions between excessive manganese exposures and dietary iron-deficiency in neurodegeneration, *Environ. Toxicol. Pharmacol.*, 2005, **19**, 415–421, DOI: 10.1016/j.etap.2004.12.053.

62 (*a*) J. Salazar, N. Mena, S. Hunot, A. Prigent, D. Alvarez-Fischer, M. Arredondo, C. Duyckaerts, V. Sazdovitch, L. Zhao, L. M. Garrick, M. T. Nunez, M. D. Garrick, R. Raisman-Vozari and E. C. Hirsch, Divalent metal transporter 1 (DMT1) contributes to neurodegeneration in animal models of Parkinson's disease, *Proc. Natl. Acad. Sci. U. S. A.*, 2008, **105**, 18578–18583, DOI: 10.1073/pnas.0804373105; (*b*) V. A. Fitsanakis, N. Zhang, M. J. Avison, K. M. Erikson, J. C. Gore and M. Aschner, Changes in dietary iron exacerbate regional brain manganese accumulation as determined by magnetic resonance imaging, *Toxicol. Sci.*, 2011, **120**, 146–153, DOI: 10.1093/toxsci/kfq376.

63 (*a*) R. D. Snyder and M. B. Friedman, Enhancement of cytotoxicity and clastogenicity of l-DOPA and dopamine by manganese and copper, *Mutat. Res.*, 1998, **405**, 1–8;

Published on 12 December 2013. Downloaded on 30/01/2014 17:07:09.

(*b*) S. C. Sistrunk, M. K. Ross and N. M. Filipov, Direct effects of manganese compounds on dopamine and its metabolite Dopac: an in vitro study, *Environ. Toxicol. Pharmacol.*, 2007, **23**, 286–296, DOI: 10.1016/j.etap.2006.11.004.

64 J. Park, S. B. Lee, S. Lee, Y. Kim, S. Song, S. Kim, E. Bae, J. Kim, M. Shong, J. M. Kim and J. Chung, Mitochondrial dysfunction in Drosophila PINK1 mutants is complemented by parkin, *Nature*, 2006, **441**, 1157–1161, DOI: 10.1038/nature04788.

65 A. Miyama, Y. Saito, K. Yamanaka, K. Hayashi, T. Hamakubo and N. Noguchi, Oxidation of DJ-1 induced by 6-hydroxydopamine decreasing intracellular glutathione, *PLoS One*, 2011, **6**, e27883, DOI: 10.1371/journal.pone.0027883.

66 (*a*) P. Moi, K. Chan, I. Asunis, A. Cao and Y. W. Kan, Isolation of NF-E2-related factor 2 (Nrf2), a NF-E2-like basic leucine zipper transcriptional activator that binds to the tandem NF-E2/AP1 repeat of the beta-globin locus control region, *Proc. Natl. Acad. Sci. U. S. A.*, 1994, **91**, 9926–9930; (*b*) M. McMahon, K. Itoh, M. Yamamoto and J. D. Hayes, Keap1-dependent proteasomal degradation of transcription factor Nrf2 contributes to the negative regulation of antioxidant response element-driven gene expression, *J. Biol. Chem.*, 2003, **278**, 21592–21600, DOI: 10.1074/jbc.M300931200.

67 J. H. An and T. K. Blackwell, SKN-1 links C. elegans mesendodermal specification to a conserved oxidative stress response, *Genes Dev.*, 2003, **17**, 1882–1893, DOI: 10.1101/gad.1107803.

68 Y. Imaizumi, Y. Okada, W. Akamatsu, M. Koike, N. Kuzumaki, H. Hayakawa, T. Nihira, T. Kobayashi, M. Ohyama, S. Sato, M. Takanashi, M. Funayama, A. Hirayama, T. Soga, T. Hishiki, M. Suematsu, T. Yagi, D. Ito, A. Kosakai, K. Hayashi, M. Shouji, A. Nakanishi, N. Suzuki, Y. Mizuno, N. Mizushima, M. Amagai, Y. Uchiyama, H. Mochizuki, N. Hattori and H. Okano, Mitochondrial dysfunction associated with increased oxidative stress and alpha-synuclein accumulation in PARK2 iPSC-derived neurons and postmortem brain tissue, *Mol. Brain*, 2012, **5**, 35, DOI: 10.1186/1756-6606-5-35.

69 C. M. Clements, R. S. McNally, B. J. Conti, T. W. Mak and J. P. Ting, DJ-1, a cancer- and Parkinson's disease-associated protein, stabilizes the antioxidant transcriptional master regulator Nrf2, *Proc. Natl. Acad. Sci. U. S. A.*, 2006, **103**, 15091–15096, DOI: 10.1073/pnas0607260103.

70 Y. Suzuki, T. Mouri, K. Nishiyama and N. Fujii, Study of subacute toxicity of manganese dioxide in monkeys, *Tokushima J. Exp. Med.*, 1975, **22**, 5–10.

71 (*a*) J. Xu, S. Y. Kao, F. J. Lee, W. Song, L. W. Jin and B. A. Yankner, Dopamine-dependent neurotoxicity of alpha-synuclein: a mechanism for selective neurodegeneration in Parkinson disease, *Nat. Med.*, 2002, **8**, 600–606, DOI: 10.1038/nm0602-600; (*b*) C. J. Choong and Y. H. Say, Neuroprotection of alpha-synuclein under acute and chronic rotenone and maneb treatment is abolished by its familial Parkinson's disease mutations A30P, A53T and E46K, *Neurotoxicology*, 2011, **32**, 857–863, DOI: 10.1016/j.neuro.2011.05.012; (*c*) A. Sidhu, C. Wersinger, C. E. Moussa and P. Vernier, The role of alpha-synuclein in both neuroprotection and neurodegeneration, *Ann. N. Y. Acad. Sci.*, 2004, **1035**, 250–270, DOI: 10.1196/annals.1332.016.

72 (*a*) J. M. George, The synucleins, *Genome Biol.*, 2002, **3**, 243–254, REVIEWS3002; (*b*) D. F. Clayton and J. M. George, The synucleins: a family of proteins involved in synaptic function, plasticity, neurodegeneration and disease, *Trends Neurosci.*, 1998, **21**, 249–254, DOI: S0166-2236(97)01213-7.

73 D. R. Brown, Interactions between metals and alpha-synuclein–function or artefact?, *FEBS J.*, 2007, **274**, 3766–3774, DOI: 10.1111/j.1742-4658.2007.05917.x.

74 (*a*) A. Binolfi, R. M. Rasia, C. W. Bertoncini, M. Ceolin, M. Zweckstetter, C. Griesinger, T. M. Jovin and C. O. Fernandez, Interaction of alpha-synuclein with divalent metal ions reveals key differences: a link between structure, binding specificity and fibrillation enhancement, *J. Am. Chem. Soc.*, 2006, **128**, 9893–9901, DOI: 10.1021/ja0618649; (*b*) A. Santner and V. N. Uversky, Metalloproteomics and metal toxicology of alpha-synuclein, *Metallomics*, 2010, **2**, 378–392, DOI: 10.1039/b926659c.

75 (*a*) M. Bisaglia, I. Tessari, S. Mammi and L. Bubacco, Interaction between alpha-synuclein and metal ions, still looking for a role in the pathogenesis of Parkinson's disease, *NeuroMol. Med.*, 2009, **11**, 239–251, DOI: 10.1007/s12017-009-8082-1; (*b*) A. Ahmad, C. S. Burns, A. L. Fink and V. N. Uversky, Peculiarities of copper binding to alpha-synuclein, *J. Biomol. Struct. Dyn.*, 2012, **29**, 825–842, DOI: 10.1080/073911012010525023.

76 (*a*) V. N. Uversky, J. Li and A. L. Fink, Metal-triggered structural transformations, aggregation, and fibrillation of human alpha-synuclein. A possible molecular NK between Parkinson's disease and heavy metal exposure, *J. Biol. Chem.*, 2001, **276**, 44284–44296, DOI: 10.1074/jbc.M105343200; (*b*) T. Verina, J. S. Schneider and T. R. Guilarte, Manganese exposure induces alpha-synuclein aggregation in the frontal cortex of non-human primates, *Toxicol. Lett.*, 2013, **217**, 177–183, DOI: 10.1016/j.toxlet.2012.12.006.

77 P. Davies, D. Moualla and D. R. Brown, Alpha-synuclein is a cellular ferrireductase, *PLoS One*, 2011, **6**, e15814, DOI: 10.1371/journal.pone.0015814.

78 (*a*) K. Melachroinou, M. Xilouri, E. Emmanouilidou, R. Masgrau, P. Papazafiri, L. Stefanis and K. Vekrellis, Deregulation of calcium homeostasis mediates secreted alpha-synuclein-induced neurotoxicity, *Neurobiol. Aging*, 2013, **34**, 2853–2865, DOI: 10.1016/j.neurobiolaging.2013.06.006; (*b*) E. Emmanouilidou, L. Stefanis and K. Vekrellis, Cell-produced alpha-synuclein oligomers are targeted to, and impair, the 26S proteasome, *Neurobiol. Aging*, 2010, **31**, 953–968, DOI: 10.1016/j.neurobiolaging.2008.07.008.

79 F. Pan-Montojo, M. Schwarz, C. Winkler, M. Arnhold, G. A. O'Sullivan, A. Pal, J. Said, G. Marsico, J. M. Verbavatz, M. Rodrigo-Angulo, G. Gille, R. H. Funk and H. Reichmann, Environmental toxins trigger PD-like progression via increased alpha-synuclein release from enteric neurons in mice, *Sci. Rep.*, 2012, **2**, 898, DOI: 10.1038/srep00898.

80 M. Lee, D. Hyun, B. Halliwell and P. Jenner, Effect of the overexpression of wild-type or mutant alpha-synuclein on cell susceptibility to insult, *J. Neurochem.*, 2001, **76**, 998–1009.

81 (*a*) S. Shimada, S. Kitayama, C. L. Lin, A. Patel, E. Nanthakumar, P. Gregor, M. Kuhar and G. Uhl, Cloning and expression of a cocaine-sensitive dopamine transporter complementary DNA, *Science*, 1991, **254**, 576–578; (*b*) W. A. Cass, N. R. Zahniser, K. A. Flach and G. A. Gerhardt, Clearance of exogenous dopamine in rat dorsal striatum and nucleus accumbens: role of metabolism and effects of locally applied uptake inhibitors, *J. Neurochem.*, 1993, **61**, 2269–2278; (*c*) J. E. Kilty, D. Lorang and S. G. Amara, Cloning and expression of a cocaine-sensitive rat dopamine transporter, *Science*, 1991, **254**, 578–579.

82 (*a*) M. Huotari, M. Santha, L. R. Lucas, M. Karayiorgou, J. A. Gogos and P. T. Mannisto, Effect of dopamine uptake inhibition on brain catecholamine levels and locomotion in catechol-O-methyltransferase-disrupted mice, *J. Pharmacol. Exp. Ther.*, 2002, **303**, 1309–1316, DOI: 10.1124/jpet.102.043042; (*b*) P. W. McDonald, S. L. Hardie, T. N. Jessen, L. Carvelli, D. S. Matthies and R. D. Blakely, Vigorous motor activity in Caenorhabditis elegans requires efficient clearance of dopamine mediated by synaptic localization of the dopamine transporter DAT-1, *J. Neurosci.*, 2007, **27**, 14216–14227, DOI: 10.1523/JNEUROSCI.2992-07.2007.

Published on 12 December 2013. Downloaded on 30/01/2014 17:07:09.